Improvement of well-posedness of SPACE code using the one-dimensional turbulence term

Byoung Jae Kim [a], Young Seock An[a], Kyung Doo Kim[b*]
[a]*School of Mechanical Engineering, Chungnam National University, Daejeon*
[b]*Thermal-Hydraluics and Severe Accident Research Division, Korea Atomic Energy Research Institute, Daejeon*
[*]*Corresponding author: kdkim@kaeri.re.kr*

1. Introduction

Many efforts have been made to improve the well-posedness of one-dimensional two-fluid equations. Examples include numerical/artificial/material viscosity, interfacial pressure, virtual mass, gravity effect, surface tension, etc. However, none is perfect in terms of physics; each model has its own drawback or is applicable to the limited flow patterns.

[1] investigated the numerical stability of two-fluid equations with material viscous terms. While the inclusion of the viscosity rendered the governing differential equations well-posed, no obvious improvement in numerical stability was found. The reason is the material viscosity terms are small. Recently, [2,3] demonstrated the improved well-posedness by adding the second-derivative terms in the mass and momentum equations. In particular, they considered turbulent viscous terms and showed excellent improvement of well-posedness. However, the problem is that the mass is not strictly conserved since the mass source terms are not zero.

For this reason, the present study incorporates the turbulent viscous terms only into the momentum equations of the SPACE code. Two standard problems are simulated.

2. Theory

2.1 Governing equations

For adiabatic, incompressible, and one-dimensional flows, the two-fluid mass equations are

$$\frac{\partial \alpha_g}{\partial t}+\frac{\partial}{\partial x}(\alpha_g u_g)=0\,, \tag{1}$$

$$\frac{\partial \alpha_l}{\partial t}+\frac{\partial}{\partial x}(\alpha_l u_l)=0\,. \tag{2}$$

The two-fluid momentum equations are given by

$$\alpha_g\rho_g\left(\frac{\partial u_g}{\partial t}+u_g\frac{\partial u_g}{\partial x}\right)=-\alpha_g\frac{\partial p}{\partial x}+\mu_g^{eff}\frac{\partial}{\partial x}\left(\alpha_g\frac{\partial u_g}{\partial x}\right), \tag{3}$$

$$\alpha_l\rho_l\left(\frac{\partial u_l}{\partial t}+u_l\frac{\partial u_l}{\partial x}\right)=-\alpha_l\frac{\partial p}{\partial x}+\mu_l^{eff}\frac{\partial}{\partial x}\left(\alpha_l\frac{\partial u_l}{\partial x}\right). \tag{4}$$

The last terms in Eqs. (3) and (4) originate from the material and turbulence viscosities. μ_g^{eff} is the sum of the material and turbulence viscosities for the gas phase. The same goes to the liquid phase. In general, the last terms are neglected on the basis that the axial component of the shear stress is negligible compared to the inherent numerical viscosity. However, for unstable two-fluid models these terms are of central importance, especially flor convergence analyses.

The last two terms in Eqs. (3) and (4) may seem similar to the artificial viscosity terms in RELAP5[4]. However, those two terms are proportional to the sum of the material and turbulence viscosities, while the artificial viscosities in RELAP5 are simply relative to the phasic densities.

2.2 Stability analysis

Equations (1)~(4) can be written in the following matrix form:

$$\mathbf{A}\frac{\partial \mathbf{\Psi}}{\partial t}+\mathbf{B}\frac{\partial \mathbf{\Psi}}{\partial x}+\mathbf{C}\frac{\partial^2 \mathbf{\Psi}}{\partial x^2}=0\,, \tag{5}$$

where $\mathbf{\Psi}=(\alpha \quad u_g \quad u_l \quad p)$, and

$$\mathbf{A}=\begin{pmatrix}1&0&0&0\\-1&0&0&0\\0&1&0&0\\0&0&1&0\end{pmatrix}, \tag{6}$$

$$\mathbf{B}=\begin{pmatrix}u_g&\alpha_g&0&0\\-u_l&0&1-\alpha_g&0\\0&u_g&0&1/\rho_g\\0&0&u_l&1/\rho_l\end{pmatrix}, \tag{7}$$

$$\mathbf{C}=\begin{pmatrix}0&0&0&0\\0&0&0&0\\0&-\mu_g^{eff}/\rho_g&0&0\\0&0&-\mu_l^{eff}/\rho_l&0\end{pmatrix}. \tag{8}$$

According to the stability analysis, the following relation must be satisfied so as the solution to be non-trivial.

$$|\,\omega\mathbf{A}-k\mathbf{B}-ik^2\mathbf{C}\,|=0\,. \tag{9}$$

Therefore, one obtains the growth rate as follows:

$$\mathrm{Im}[\omega]=-\frac{\nu}{2}k^2+\sqrt{\frac{\alpha_g\alpha_l\rho_g\rho_l(u_g-u_l)^2k^2}{(\alpha_l\rho_g+\alpha_g\rho_l)^2}+\frac{\nu^2k^4}{4}}\,. \tag{10}$$

$\mathrm{Im}[\,\omega\,]$ takes the imaginary part of the complex growth rate ω. In deriving that result, $\nu=\mu_g^{eff}/\rho_g=\mu_l^{eff}/\rho_l$ has been assumed. For $\nu=0$, Eq. (10) goes to the existing result:

$$\mathrm{Im}[\omega]=\frac{\sqrt{\alpha_g\alpha_l\rho_g\rho_l}}{\alpha_l\rho_g+\alpha_g\rho_l}\,|\,u_g-u_l\,|\,k\,. \tag{11}$$

This implies that the equation system is unstable for all wavenumbers. However, for $\nu \neq 0$, Im[ω] is positive but it goes to zero as $k \to \infty$. In other words, the equation system is greatly stabilized for short waves. The present result differs from [1,2] in that the mass is strictly conserved.

3. Results and discussion

3.1 Water-faucet flow

The water-faucet problem describes the free fall of a column of water and has been used as a standard benchmark problem for many two-fluid model codes.

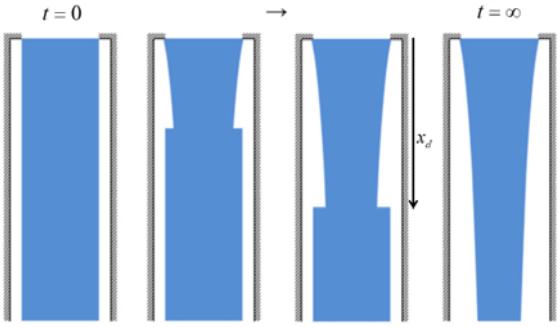

Fig. 1. Development of the water profile

Initially, the liquid fraction and velocity are uniform as $\alpha_{l0} = 0.8$ and $u_{l0} = 10$ m/s. The fluids are the water and air at 300 K under 1 atm. Neglecting all frictions, the theoretical distance, liquid velocity, and liquid fraction are

$$x_d = u_{l0}t + 0.5gt^2, \tag{12}$$

$$u_l(t,x) = \begin{cases} \sqrt{u_{l0}^2 + 2gx}, & x < x_d \\ u_{l0} + gt, & x \geq x_d \end{cases}, \tag{13}$$

$$\alpha_l(x,t) = \begin{cases} \alpha_{l0}u_{l0} / u_l, & x < x_d \\ \alpha_{l0}, & x \geq x_d \end{cases}. \tag{14}$$

Figure 2 shows the SPACE code nodding. The total length of the pipe is 6.0 m and the diameter is 1 m. Figure 3 shows the liquid fraction profiles depending on N, the number of cells in the pipe. For small mesh sizes of N = 500 and 950, unphysical profiles are predicted. This is because the existing two-fluid equation system is ill-posed; very unstable for short waves. Figure 4 shows the evolution of the liquid profile as a function of time. Overshoots are seen after about 0.3 s.

Figures 5 and 6 show the results when the turbulent viscosity terms are included in the momentum equations:

$$\nu = \frac{1}{2\pi}\frac{\sqrt{\alpha_g\alpha_l\rho_g\rho_l}}{\alpha_l\rho_g + \alpha_g\rho_l}(2D)\,|\,u_g - u_l\,|. \tag{15}$$

Equation (15) is based on the critical condition for separated flows. One can see that overshoots are greatly suppressed in the discontinuous region; the liquid profiles are smooth across the discontinuous region.

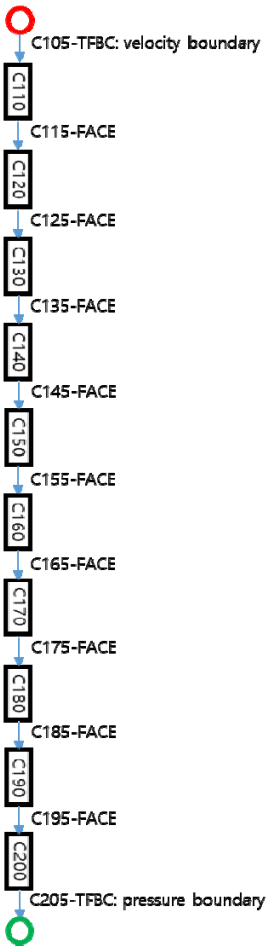

Fig. 2 SPACE code nodding for the water-faucet flow

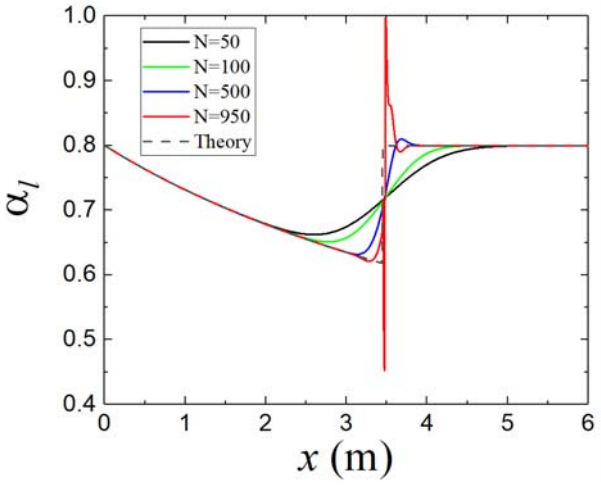

Fig. 3 Simulation result at $t = 0.3$ s for $\nu = 0$ (water-faucet)

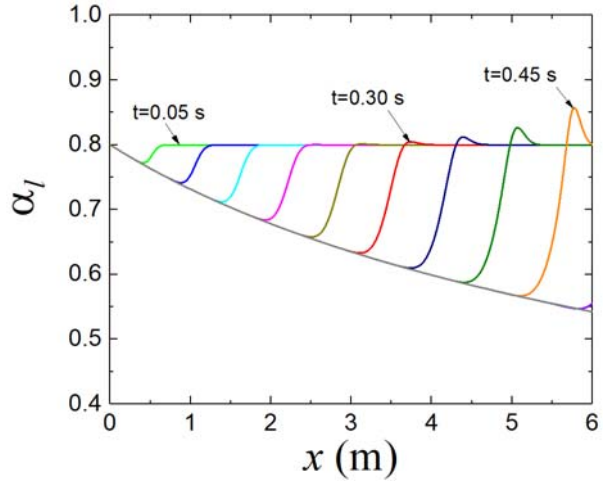

Fig. 4 Simulation results for $\nu = 0$ (water-faucet)

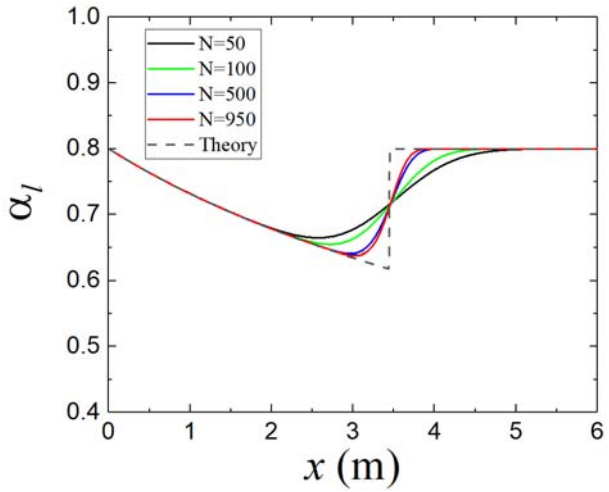

Fig. 5 Simulation result at $t = 0.3$ s for $\nu \neq 0$ (water-faucet)

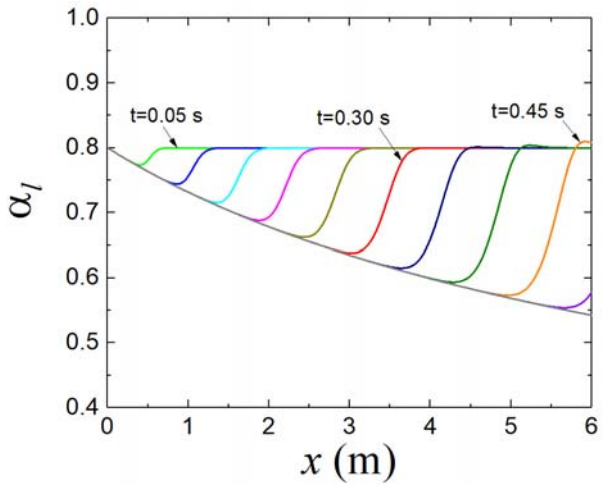

Fig. 6 Simulation results for $\nu \neq 0$ (water-faucet)

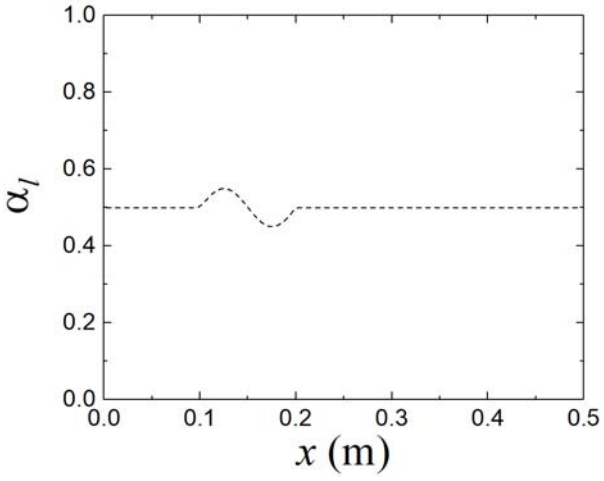

Fig. 8 Initial water fraction profile (torus)

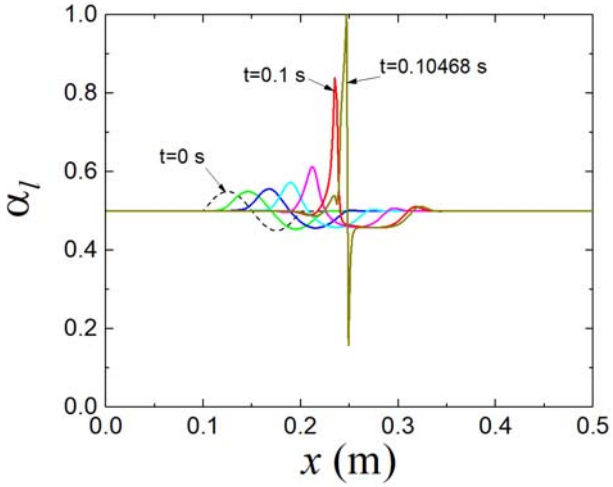

Fig. 9 Simulation results for $\nu = 0$ and $N = 250$ (torus)

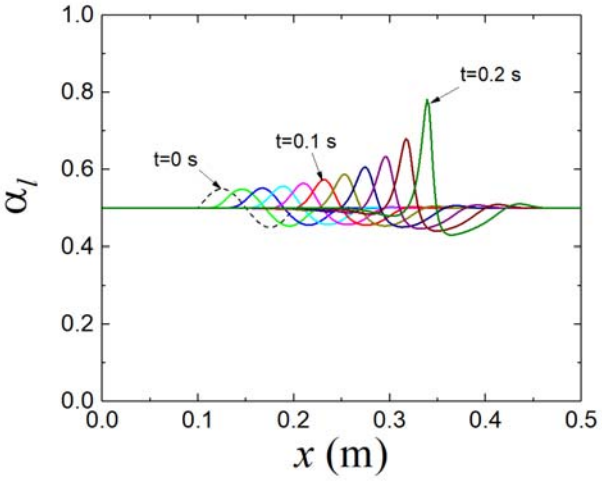

Fig. 10 Simulation results for $\nu \neq 0$ and $N = 250$ (torus)

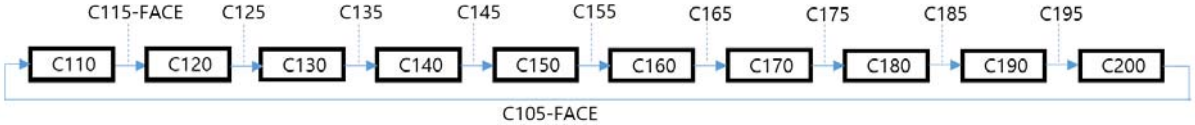

Fig. 7 SPACE nodding for horizontal torus flow

3.2 Horizontal torus flow

We now consider a horizontally-stratified flow. Figure 7 show the SPACE code nodding for a horizontal pipe with the total length of 0.5 m and the diameter of 0.03 m. The two ends are connected, i.e., torus geometry. Initially, the water velocity $u_l = 1.0$ m/s, the air velocity $u_g = 13.0$ m/s, and the pipe is filled with water as shown in Fig. 8. The temperature is 300 K and the pressure is 1 atm. At this condition, the flow is unstable in view of the Kelvin-Helmholtz instability. The critical relative velocity for instability is 11.3 m/s, but the initial relative velocity is $u_g - u_l = 13$ m/s .

Figure 9 shows the evolution of the liquid profile as a function of time when the turbulent viscosity is not included and the number of cells is 250. The flow is considerably unstable for the small mesh size and the calculation is terminated at t=0.10468 s. Figure 10 shows the result when the turbulent viscosity is included. The evolution of the liquid profile is predicted smoothly. This excellent result is due to the turbulent viscosity terms.

3. Conclusions

One-dimensional turbulent viscosity terms were included in the two-fluid momentum equations. No treatment was applied to the mass equations. The water-faucet and horizontal torus problems demonstrated the improvement of the well-posedness. The present approach differs from [1,2], in the mass conservation. At present, we are investigating the effect of the mass conservation modifying the mass source terms.

Acknowledgement

This work was supported by the Korea Institute of Energy Technology Evaluation and Planning(KETEP) and the Ministry of Trade, Industry & Energy(MOTIE) of the Republic of Korea (No.20161510101840).

REFERENCES

[1] J. M. Doster and M. A. Holmes, “Numerical stability of the six-equation, single-pressure model with viscous terms,” Nuclear Science and Engineering, Vol.124, pp.125-144, 1996.
[2] W. Fullmer, V. H. Ransom, and M. A. L. Bertodano, “Linear and nonlinear analysis of an unstable, but well-posed, one-dimensional two-fluid model for two-phase flow based on the inviscid Kelvin-Helmholtz instability,” Nuclear Engineering and Design, Vol. 268, pp.173-184, 2014a.
[3] W. Fullmer, S. Y. Lee, and M. A. L. Bertodano, “An Artificial viscosity for the ill-posed one-dimensional incompressible two-fluid model,” Nuclear Technology, Vol. 185, pp.296-308, 2014b.
[4] “RELAP5-3D Code manual: I. Code structure, system models, and solution methods,” INEEL-EXT-98-00834, Revision 4.0, 2012.